Neurobiology of Disease 153 (2021) 105304

Contents lists available at ScienceDirect

Neurobiology of Disease

journal homepage: www.elsevier.com/locate/ynbdi

A $GABA_B$ receptor antagonist rescues functional and structural impairments in the perirhinal cortex of a mouse model of CDKL5 deficiency disorder

Laura Gennaccaro [a,1], Claudia Fuchs [a,1], Manuela Loi [a,2], Vincenzo Roncacè [b,2], Stefania Trazzi [a], Yassine Ait-Bali [c,2], Giuseppe Galvani [a], Anna Cecilia Berardi [b], Giorgio Medici [a], Marianna Tassinari [a], Elisa Ren [a], Roberto Rimondini [d], Maurizio Giustetto [c], Giorgio Aicardi [b,**], Elisabetta Ciani [a,*]

[a] Department of Biomedical and Neuromotor Science, University of Bologna, Bologna, Italy
[b] Department for Life Quality Studies, University of Bologna, Bologna, Italy
[c] Department of Neuroscience "Rita Levi Montalcini", University of Turin, Turin, Italy
[d] Department of Medical and Clinical Sciences, University of Bologna, Bologna, Italy

ARTICLE INFO

Keywords:
CDKL5
Synaptic plasticity
Dendritic pattern
Perirhinal cortex
GABAergic transmission

ABSTRACT

CDKL5 (cyclin-dependent kinase-like 5) deficiency disorder (CDD) is a severe neurodevelopmental encephalopathy characterized by early-onset epilepsy and intellectual disability. Studies in mouse models have linked CDKL5 deficiency to defects in neuronal maturation and synaptic plasticity, and disruption of the excitatory/inhibitory balance. Interestingly, increased density of both GABAergic synaptic terminals and parvalbumin inhibitory interneurons was recently observed in the primary visual cortex of *Cdkl5* knockout (KO) mice, suggesting that excessive GABAergic transmission might contribute to the visual deficits characteristic of CDD. However, the functional relevance of cortical GABAergic circuits abnormalities in these mutant mice has not been investigated so far. Here we examined GABAergic circuits in the perirhinal cortex (PRC) of *Cdkl5* KO mice, where we previously observed impaired long-term potentiation (LTP) associated with deficits in novel object recognition (NOR) memory. We found a higher number of GABAergic (VGAT)-immunopositive terminals in the PRC of *Cdkl5* KO compared to wild-type mice, suggesting that increased inhibitory transmission might contribute to LTP impairment. Interestingly, while exposure of PRC slices to the $GABA_A$ receptor antagonist picrotoxin had no positive effects on LTP in *Cdkl5* KO mice, the selective $GABA_B$ receptor antagonist CGP55845 restored LTP magnitude, suggesting that exaggerated $GABA_B$ receptor-mediated inhibition contributes to LTP impairment in mutants. Moreover, acute *in vivo* treatment with CGP55845 increased the number of PSD95 positive puncta as well as density and maturation of dendritic spines in PRC, and restored NOR memory in *Cdkl5* KO mice. The present data show the efficacy of limiting excessive $GABA_B$ receptor-mediated signaling in improving synaptic plasticity and cognition in CDD mice.

Abbreviations: BDNF, brain-derived neurotrophic factor; CDD, CDKL5 deficiency disorder; CDKL5, Cyclin-dependent kinase-like 5; *Cdkl5* KO mice, *Cdkl5* knockout mice; CGP, CGP55845; fEPSPs, field excitatory postsynaptic potentials; GABA, gamma-aminobutyric acid; $GABA_B$Rs, $GABA_B$ receptors; GAD67, glutamic acid decarboxylase 67; GAPDH, Glyceraldehyde 3-phosphate dehydrogenase; GIRK2, G protein-coupled inwardly-rectifying potassium channels 2; LTP, Long-term potentiation; NMDA, *N*-Nitrosodimethylamine; NOR, novel object recognition; OD, Mean optical density; PBS, phosphate-buffered saline; Picro, picrotoxin; PPR, paired-pulse ratio; PRC, perirhinal cortex; PSD95, postsynaptic density protein 95; RT-qPCR, quantitative reverse transcription PCR; SEM, standard error of mean; TBS, theta burst stimulation; TrkB, tyrosine kinase receptor B; VGAT, GABA vesicular transporter..

* Corresponding author at: Department of Biomedical and Neuromotor Sciences, University of Bologna, Piazza di Porta San Donato 2, 40126 Bologna, Italy.
** Corresponding author at: Department for Life Quality Studies, University of Bologna, Via San Donato 19/2, 40127 Bologna, Italy.
E-mail addresses: giorgio.aicardi@unibo.it (G. Aicardi), elisabetta.ciani@unibo.it (E. Ciani).
[1] Authors labeled with 1 or 2 contributed equally to the work.
[2] Y.A-B. present address: Department of Biology, Higher Normal School, University Mohamed V, Rabat, Morocco.

https://doi.org/10.1016/j.nbd.2021.105304
Received 17 November 2020; Received in revised form 16 February 2021; Accepted 17 February 2021
Available online 20 February 2021

1. Introduction

Mutations in the X-linked gene encoding cyclin dependent kinase like 5 (CDKL5) are the cause of a severe rare neurological disorder recently named CDKL5 deficiency disorder (CDD), which results in early onset seizures that are difficult to control and severe intellectual disability. CDD patients also display impaired vision and motor skills, and breathing disturbance (Bertani et al., 2006; Demarest et al., 2019a; Demarest et al., 2019b; Fehr et al., 2013; Guerrini and Parrini, 2012; Mari et al., 2005). Mice with genetically altered *Cdkl5,* such as the *Cdkl5* knockout (KO), provide powerful tools for the investigation of CDD pathophysiology (Amendola et al., 2014; Okuda et al., 2017; Tang et al., 2017; Wang et al., 2012). *Cdkl5* KO mice recapitulate a number of behavioral and physiological features of CDD, including deficits in cognition, visual impairment, and irregular breathing (Amendola et al., 2014; Fuchs et al., 2015; Lo Martire et al., 2017; Mazziotti et al., 2017; Ren et al., 2019; Trazzi et al., 2018; Wang et al., 2012).

The neurological symptoms associated with CDD along with the abundant expression of CDKL5 in the brain (Hector et al., 2016; Montini et al., 1998) suggest that CDKL5 plays a role in brain development and function. Moreover, its localization in mature neurons within different subcellular compartments, including the nucleus and dendritic spines (Chen et al., 2010; Ricciardi et al., 2012; Rusconi et al., 2008), implies that CDKL5 plays multiple roles by regulating distinct signaling pathways. Recent studies using *Cdkl5* KO neurons and mice have demonstrated that CDKL5 regulates axon outgrowth (Nawaz et al., 2016) and dendritic morphogenesis (Amendola et al., 2014; Chen et al., 2010; Fuchs et al., 2015; Fuchs et al., 2014). Increasing evidence also suggests that CDKL5 plays a role in excitatory synapse development and function in the adult brain. A significant reduction in spine density and in the number of mature spines in the hippocampus, cerebral cortex, and thalamus of *Cdkl5* KO mice (Della Sala et al., 2016; Lupori et al., 2019; Pizzo et al., 2016; Pizzo et al., 2020; Ren et al., 2019; Trazzi et al., 2016) implies a reduction in the excitatory synaptic inputs that may contribute to the impairment of activity-dependent synaptic plasticity observed in the somatosensory (Della Sala et al., 2016) and perirhinal (Ren et al., 2019) cortex.

Since *Cdkl5* is expressed at high levels in inhibitory interneurons (Rusconi et al., 2008), the change in the excitatory/inhibitory balance in the CDKL5-deficient brain that alters synaptic plasticity and triggers learning and memory deficits might also depend on altered inhibitory interneuron function. Recent studies have shown that CDKL5 deficiency resulted in an increase in the inhibitory synaptic marker VGAT (Lupori et al., 2019; Pizzo et al., 2016) and in the density of parvalbumin inhibitory interneurons in the primary visual cortex (Pizzo et al., 2016), suggesting an enhancement of GABAergic transmission that might contribute to the visual deficits characteristic of CDD. However, the relationship between GABAergic abnormalities in the cerebral cortex and the functional deficits observed in these mice has not been investigated so far.

In a recent study in *Cdkl5* KO mice, we found that long-term potentiation (LTP) is impaired in the perirhinal cortex (PRC) (Ren et al., 2019), an association cortex that is crucial for recognition memory (Brown and Aggleton, 2001). This functional deficit was associated with reduced spine density and maturation and impairment of novel object recognition (NOR) memory (Ren et al., 2019). Inhibition mediated by $GABA_B$ receptors in the PRC plays a major role in the regulation of neuronal excitability in a frequency-dependent manner (Ziakopoulos et al., 2000), and may be critical for recognition memory formation. Thus, in the present study we examined the effect of GABAergic transmission inhibition in the PRC of *Cdkl5 KO* mice. We found that *in vitro* exposure to a $GABA_B$ receptor antagonist rescued defective LTP in PRC slices, and acute *in vivo* treatment with the same antagonist increased the number of PSD95 positive puncta and the number and maturation of dendritic spines in PRC, and restored NOR memory.

2. Materials and methods

2.1. Animal husbandry

The mice used in this work derive from the *Cdkl5* KO strain in the C57BL/6 N background developed in (Amendola et al., 2014) and backcrossed in C57BL/6 J for three generations. Hemizygous *Cdkl5* KO (−/Y) mice were produced and karyotyped as described (Amendola et al., 2014). Age-matched wild-type (+/Y) littermates were used for all experiments. The day of birth was designated as postnatal day (P) zero and animals with 24 h of age were considered as 1-day-old animals (P1). Mice were housed 3–5 per cage on a 12 h light/dark cycle in a temperature- (23 °C) and humidity-controlled environment with standard mouse chow and water *ad libitum*. The animals' health and comfort were controlled by the veterinary service. All research and animal care procedures were performed according to protocols approved by the Italian Ministry for Health and by the Bologna University Bioethical Committee. All efforts were made to minimize animal suffering and to keep the number of animals used to a minimum.

2.2. Experimental protocol

Experiments were carried out on 2-month-old *Cdkl5* +/Y and *Cdkl5* -/Y male mice. Treated animals received a single intraperitoneal injection of CGP55845 (0.5 mg/kg suspended in saline, 10 mL/kg), or saline only. The dosage of 0.5 mg/kg CGP55845 was chosen on the basis of previous studies (Kleschevnikov et al., 2012). Two hours after treatment mice were behaviorally tested and subsequently sacrificed for histological analyses.

2.3. RNA isolation and RT-qPCR

RNA isolation and RT-qPCR were conducted on *Cdkl5* +/Y ($n = 8$) and *Cdkl5* -/Y (n = 8) mice. Animals were euthanized with isoflurane (2% in pure oxygen) and sacrificed through cervical dislocation. The brain was quickly removed, and the cortex underwent mRNA isolation using the TRI Reagent method according to the manufacturer's instructions (Sigma-Aldrich, St. Louis, MO, USA). cDNA synthesis was achieved with 2 μg of total RNA using iScript™ Advanced cDNA Synthesis Kit (Bio-Rad, Hercules, CA, USA) according to the manufacturer's instructions. Real-time PCR was performed using SsoAdvanced Universal SYBR Green Supermix (Bio-Rad) in an iQ5 Real-Time PCR Detection System (Bio-Rad). We used primer pairs (Supplementary table 1) that gave an efficiency close to 100%. Glyceraldehyde 3-phosphate dehydrogenase (GAPDH) was used as a reference gene for normalization in the qPCR. Relative quantification was performed using the ΔΔCt method (Livak and Schmittgen, 2001).

2.4. Histological analysis

Histological analyses were conducted on behaviorally naïve animals (immunohistochemistry for VGAT and gephyrin) or vehicle/CGP55845-treated mice 1 h after behavioral testing (Golgi staining and immunohistochemistry for the scaffolding postsynaptic density protein 95, PSD95). Animals were euthanized with isoflurane (2% in pure oxygen) and sacrificed through cervical dislocation. Brains were quickly removed and cut along the midline. Right hemispheres were fixed *via* immersion in 4% paraformaldehyde in 100 mM phosphate buffer, pH 7.4, stored in fixative for 48 h, kept in 20% sucrose for an additional 24 h, and then frozen with cold ice. Right hemispheres were cut with a freezing microtome into 30 μm-thick coronal sections that were serially collected in anti-freeze solution (30% glycerol; 30% ethylen-glycol; 10% PBS10X; 0.02% sodium azide; MilliQ to volume) and processed for immunohistochemistry procedures as described below. Left hemispheres were Golgi-stained as described below. For $GABA_BR$ immunofluorescence, animals were anesthetized with an intraperitoneal

injection of Avertine (Sigma-Aldrich) and transcardially perfused, first with 10 mL 0.1 M PBS (pH 7.4) and then with ice-cold paraformaldehyde [4% in 0.1 M phosphate buffer (PB), pH 7.4]. After perfusion, the brains were dissected and kept in the same fixative solution overnight at 4 °C. Brains were then cryoprotected by immersion in 10, 20, and 30% sucrose-PB solutions, cut in 30 μm sections with a cryostat and stored at −20 °C in a solution containing 30% ethylene glycol and 25% glycerol until use. All steps of sectioning, imaging, and data analysis were conducted blindly to genotype and treatment.

2.5. Immunohistochemistry

After several PBS rinses, one out of every 6 free-floating serial coronal sections of the PRC were put in a blocking solution for 1 h, followed by overnight incubation at room temperature with the following primary antibodies: rabbit polyclonal anti-VGAT antibody (1:500; Synaptic System), mouse monoclonal anti-gephyrin antibody (1:500; Synaptic System), rabbit polyclonal anti-PSD95 antibody (1:1000, Abcam), guinea pig polyclonal anti-$GABA_BR$ antibody (1:2000; Chemicon). The following day, sections were washed and incubated with appropriate fluorescent secondary antibodies (1:200, Jackson ImmunoResearch Laboratories, Inc.). After several PBS rinses, the sections were mounted on gelatin-coated glass slides and coverslipped with Dako fluorescence mounting medium (Dako Italia, Milan, Italy).

For quantification of synaptic puncta, images that were processed for VGAT, gephyrin and PSD95 immunofluorescence were acquired with a Leica TCS SL confocal microscope. In each section, four images from the PRC were captured and the density of individual puncta exhibiting immunoreactivity for a specific antibody was evaluated in layers II-III, as previously described in (Pizzo et al., 2016). For the $GABA_BR$ immunosignal analysis, confocal images of the PRC were acquired in corresponding sections from six animals per genotype with a laser scanning confocal microscope (LSM5 Pascal; Zeiss, Germany) using a 40× objective, 1 μm *Z*-step (1.4 numerical aperture) and the pinhole set at 1 Airy unit. Images were background subtracted with ImageJ software (NIH, USA) using the intensity of corpus callosum background staining as threshold. Immunopositive cells were manually counted using the point tool in ImageJ software (Image processing and analysis in Java, NIH, USA). The ROI Manager tool in ImageJ software was employed to quantify integrated optical density.

2.6. Golgi staining

Left hemispheres were Golgi-stained using the FD Rapid Golgi Stain TM Kit (FD NeuroTechnologies). Briefly, hemispheres were immersed in the impregnation solution that contained mercuric chloride, potassium dichromate, and potassium chromate and stored at room temperature in darkness for 2–3 weeks. Hemispheres were cut with a microtome into 100 μm-thick coronal sections that were directly mounted onto gelatin-coated slides and were air dried at room temperature in the dark for an additional 2–3 days. After drying, sections were rinsed with distilled water and subsequently stained in the developing solution of the kit. A light microscope (Leica Mycrosystems) equipped with a motorized stage and focus control system and a color digital camera (Coolsnap-Pro; Media Cybernetics) were used to take bright field images. Measurements were carried out using Image Pro Plus software (Media Cybernetics).

2.6.1. Spine density and morphology

In Golgi-stained sections, spines of apical dendritic branches of layer II-III perirhinal neurons were acquired using a 100× oil immersion objective lens. Dendritic spine density was measured by manually counting the number of dendritic spines. In each mouse, 12–15 dendritic segments (segment length: 10 μm) from each zone were analyzed and spine density was expressed as the total number of spines per 10 μm. Based on their morphology, dendritic spines can be divided into two different categories that reflect their state of maturation: immature spines and mature spines. The number of spines belonging to each class was counted and expressed as a percentage.

2.7. Western blotting

Western blot analyses were conducted on behaviorally naïve animals. Western blotting was carried out in homogenates of the PRC. In order to obtain samples of the PRC in isolation, the brain was cut into horizontal slices (400 μm-thick) taken during the same procedure used for electrophysiological recording described below. PRC samples from 4 slices per animal gave a sufficient amount of material for western blot analysis. Total proteins were obtained as previously described (Trazzi et al., 2014). Protein concentration was determined using the Bradford method (Bradford, 1976). Equivalent amounts 50 μg of protein were subjected to electrophoresis on a BOLT Bis-Tris Plus gel (Thermo Fisher Scientific) and transferred to a Hybond ECL nitrocellulose membrane (Amersham - GE Healthcare Life Sciences). The following primary antibodies were used: rabbit polyclonal anti-VGAT antibody (1:1000; Synaptic System), mouse monoclonal anti-$GABA_BR$ antibody (1:500; Merck Millipore), rabbit polyclonal anti-GIRK2 antibody (1:500; Alomone Labs), rabbit polyclonal anti-BDNF (1:500, Santa Cruz Biotechnology), and rabbit polyclonal anti-GAPDH (1:5000, Sigma-Aldrich). HRP-conjugated goat anti-rabbit or goat anti mouse IgG (1:5000, Jackson ImmunoResearch Laboratories) secondary antibody was used. Densitometric analysis of digitized images was performed using Chemidoc XRS Imaging Systems and Image Lab™ Software (Bio-Rad).

2.8. Electrophysiology

Preparation of horizontal brain slices (400 mm-thick, including the PRC, the entorhinal cortex, and the hippocampus), electrophysiological recording of evoked field excitatory postsynaptic potentials (fEPSP), and measurement of fEPSP amplitude were performed as previously reported (Aicardi et al., 2004; Ren et al., 2019; Roncace et al., 2017). Field excitatory postsynaptic potentials (fEPSPs) evoked in layers II-III of the PRC by stimuli of increasing strength (20–220 μA) delivered at 0.033 Hz by a bipolar electrode positioned in layers II–III of the PRC (at 400–500 μm from the recording electrode, in rostral direction) were recorded to obtain input-output relations of the extracellular field potential. In LTP experiments, responses were recorded at 0.5 min intervals for 10 min before and for at least 60 min after theta burst stimulation (TBS). Stimulus intensity was adjusted to induce ~50% of the maximal synaptic response. After at least 10 min of stable baseline recording, TBS (four trains every 15 s, each train comprising 10 bursts of 5 pulses at 100 Hz, inter-burst interval 150 ms) was applied to induce LTP. LTP was defined as an increase in fEPSP amplitude of at least 10% at 25–30 min after TBS, and for the remainder of the recording (60 min after TBS). Some slices were treated with the selective antagonists for $GABA_A$ receptors (picrotoxin, 100 μM; Sigma-Aldrich) or $GABA_B$ receptors (CGP55845, 1 μM; Sigma-Aldrich) during the recording session. CGP55845 was preliminarily dissolved in concentrated aliquots and stored at −20 °C, then re-dissolved to the final concentrations in artificial cerebrospinal fluid. Picrotoxin was directly dissolved in artificial cerebrospinal fluid.

2.9. Behavioral testing

The behavioral test was performed by operators who were blind to genotype and treatment. Mice were allowed to habituate to the testing room for at least 1 h before the test. The test was performed in an open field arena (50 × 50 cm) and the behavior of the mice was monitored using a video camera placed above the center of it. The experiments were scored using EthoVision XT ver. 14 software (Noldus). Test chambers were cleaned with 70% ethanol between test subjects.

2.9.1. Pretraining habituation

The animals were habituated in an empty (without objects) open field arena for 2 days before the commencement of behavioral testing. Each animal was placed in the center of the arena and allowed to freely explore the open field for 20 min.

2.9.2. NOR task

The procedure involved a familiarization phase, followed by a preference test phase (Fig. 5A,B). In the familiarization phase (10 min duration), each animal was placed in the same arena (of the pretraining habituation), which in this phase contained four identical objects (plastic tubes, too heavy for the animal to displace; objects 1–4), each of them placed near one of the four corners of the arena (15 cm from each adjacent wall). After a delay of 1 h, during which one of the four objects (object 1) was replaced by a novel object (a wooden cube; objects 2–4 remained in the same positions), the animal was returned to the arena for the preference test phase (10 min duration; Fig. 5A,B).

Exploration behavior was measured as previously described (Ren et al., 2019). Data obtained from the 10 min of the test period are presented and a preference index of above 25% indicates the preference for an object.

2.10. Statistical analysis

If the data sets passed normality test and equal variance test, we performed Student's *t*-test or two-way ANOVA followed by Fischer or Tukey *post hoc* tests as specifically indicated in the text of each figure legend, using GraphPad Prism software (La Jolla). All values are presented as mean ± SEM, and *n* indicates the number of mice. A probability level of $p < 0.05$ was considered to be statistically significant.

3. Results

3.1. GABAergic transmission in the perirhinal cortex of Cdkl5 -/Y mice

To assess the impact of the lack of *Cdkl5* on the inhibitory circuitry, we stained for VGAT, a presynaptic marker of inhibitory synapses (Chaudhry et al., 1998). VGAT localizes to synaptic vesicles and can be taken as an index of abundance of GABAergic inhibitory terminals. In line with previous evidence in the primary visual cortex of *Cdkl5* -/Y mice (Lupori et al., 2019; Pizzo et al., 2016), we found an increased number of VGAT positive puncta (Fig. 1A,B) in the PRC of *Cdkl5* -/Y mice. Similarly, VGAT levels were higher in homogenates of the PRC from *Cdkl5* -/Y *vs.* +/Y mice (Fig. 1C,D).

To get further insight into structural changes in GABAergic inhibitory synapses, we next investigated the postsynaptic compartments. First, we analyzed the expression of gephyrin, a scaffolding protein that anchors, clusters, and stabilizes $GABA_A$ receptors at inhibitory synapses (Choii and Ko, 2015). As shown in Fig. 2A and B, we found no significant changes in the density of gephyrin-positive puncta in the PRC of *Cdkl5* -/Y mice.

Sustained inhibitory signaling in the brain, including the PRC

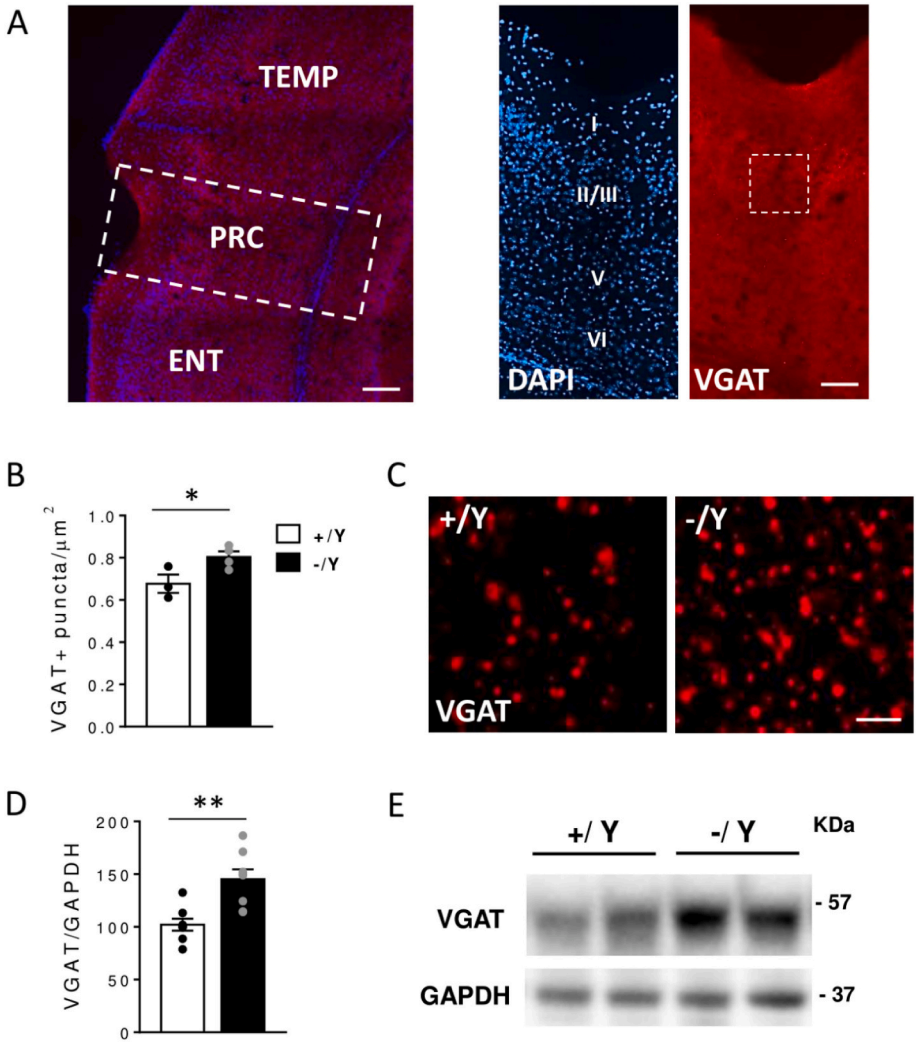

Fig. 1. Presynaptic connectivity is altered in the perirhinal cortex of *Cdkl5* -/Y mice (A) A representative image of PRC processed for fluorescent VGAT immunostaining (red) of a Cdkl5 KO (−/Y) mouse (panel on the left; scale bar = 100 µm). Nuclei are stained with Hoechst (blue). The dotted box indicates the region shown at a higher magnification in the panels on the right (scale bar = 50 µm). Roman numerals in the representative image of PRC stained for Hoechst (blue) indicate cytoarchitectonic layers. The dotted box in the representative image of PRC processed for VGAT immunostaining (red) indicates the region shown at a higher magnification in (C). (B) Number of VGAT positive puncta per μm^2 in layer II-III of the PRC of +/Y ($n = 3$ mice) and *Cdkl5* -/Y ($n = 4$ mice) mice. (C) Representative confocal images of PRC sections processed for VGAT immunohistochemistry from a *Cdkl5* +/Y mouse and a *Cdkl5* -/Y mouse. Scale bar = 2 µm. (D) Western blot analysis of VGAT level normalized to glyceraldehyde 3-phosphatedehydorgenase (GAPDH) levels in PRC of *Cdkl5* +/Y ($n = 8$ mice) and *Cdkl5* -/Y (n = 8 mice) mice. (E) Immunoblots are examples of VGAT level in PRC extracts from 2 animals of each experimental group. Values represent mean ± SEM. $^*p < 0.05$, $^{***}p < 0.001$ (Student's *t*-test).

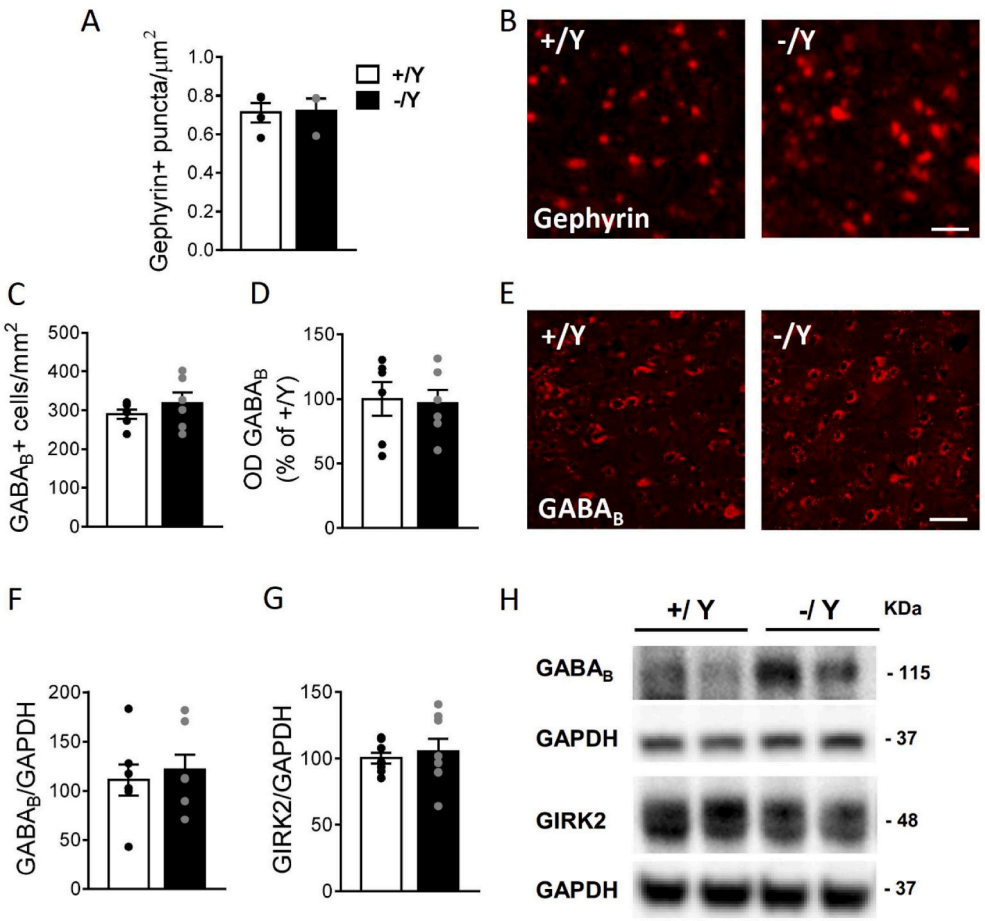

Fig. 2. Postsynaptic inhibitory connectivity is unchanged in the perirhinal cortex of *Cdkl5* -/Y mice (A) Number of gephyrin positive puncta per μm^2 in layer II-III of the PRC of +/Y (n = 4 mice) and *Cdkl5* -/Y (n = 3 mice) mice. (B) Representative confocal images of PRC sections processed for gephyrin immunohistochemistry from a *Cdkl5* +/Y mouse and a *Cdkl5* -/Y mouse. Scale bar = 2 μm. (C) Number of $GABA_B$ positive cells per mm^2 in layer II-III of the PRC of +/Y (*n* = 6 mice) and *Cdkl5* -/Y (n = 6 mice) mice. (D) Mean optical density (OD) of $GABA_B$ positive cells in the PRC of +/Y (n = 6 mice) and *Cdkl5* -/Y (n = 6 mice) mice expressed as % of the OD in *Cdkl5* +/Y mice. (E) Representative confocal images of PRC sections processed for $GABA_B$ immunohistochemistry from a *Cdkl5* +/Y mouse and a *Cdkl5* -/Y mouse. Scale bar = 25 μm. (F) Western blot analysis of $GABA_BR1$ levels normalized to GAPDH levels in the PRC of *Cdkl5* +/Y (*n* = 7 mice) and *Cdkl5* -/Y (n = 7 mice) mice. (G) Western blot analysis of GIRK2 levels normalized to GAPDH levels in the PRC of *Cdkl5* +/Y (n = 8 mice) and *Cdkl5* -/Y (n = 8 mice) mice. (H) Immunoblots are examples of $GABA_BR1$, GIRK2 and GAPDH level in PRC extracts from 2 animals of each experimental group. Values represent mean ± SEM. (Student's t-test).

(Garden et al., 2002), is mainly mediated by $GABA_B$ receptors ($GABA_BRs$) (Terunuma et al., 2014) to both the presynaptic and postsynaptic sites of glutamatergic and GABAergic neurons. We evaluated the expression levels of the $GABA_BR$ in the PRC of *Cdkl5* -/Y and +/Y mice using immunohistochemistry and western blot analysis. As shown in Fig. 2C-H, no differences in mean $GABA_BR1$ staining (Fig. 2D), in the number of $GABA_BR1$-positive cells (Fig. 2C,E), or in $GABA_BR1$ expression levels (Fig. 2F,H and Table 1) were observed. Similarly, we found no difference in the levels of GIRK2, an inward rectifying K^+ channel activated by the $GABA_B$ receptors (Fig. 2G,H), in the PRC of *Cdkl5* -/Y and +/Y mice. Again, cortical $GABA_A$ receptor subunits expression levels were not different in the PRC of *Cdkl5* -/Y and +/Y mice (Table 1).

Table 1
Expression levels of GABA receptor genes in *Cdkl5* +/Y and *Cdkl5* -/Y mice. Arbitrary values assigned for different levels of mRNA expression in cortex of *Cdkl5* -/Y (n = 8 mice) and *Cdkl5* +/Y (n = 8 mice) mice. Relative quantification was performed using the ΔΔCt method. mRNA levels in tissues obtained from *Cdkl5* +/Y mice were set to 1, and relative expression levels in *Cdkl5* -/Y mice are represented as mean ± SEM. n.s. not significant (Student's *t*-test).

	Cdkl5 +/Y	*Cdkl5* -/Y	*p*
$GABA_BR1b$	1.0 ± 0.10	0.93 ± 0.15	n.s.
$GABA_BR2$	1.0 ± 0.09	0.96 ± 0.03	n.s.
$GABA_AR1$	1.0 ± 0.09	1.35 ± 0.11	n.s.
$GABA_AR2$	1.0 ± 0.17	0.77 ± 0.05	n.s.
$GABA_AR3$	1.0 ± 0.04	1.07 ± 0.07	n.s.
$GABA_AR4$	1.0 ± 0.04	1.07 ± 0.07	n.s.
$GABA_AR5$	1.0 ± 0.14	0.90 ± 0.08	n.s.

3.2. Effect of $GABA_A$ and $GABA_B$ receptor-mediated inhibition on the input-output relations in the perirhinal cortex of Cdkl5 -/Y mice

In order to establish whether GABAergic inhibition through $GABA_A$ or $GABA_B$ receptors affects basal synaptic function, we examined the input-output relations in the superficial layers of PRC slices before and after exposure to the $GABA_A$ receptor antagonist picrotoxin (100 μM), or the $GABA_B$ receptor antagonist CGP55845 (1 μM). We found that in *Cdkl5* +/Y PRC slices exposed to picrotoxin or CGP55845 there was no increase in the magnitude of the afferent volley (Fig. 3A,C) or in that of the synaptic response (Fig. 3B,D). Similarly, in *Cdkl5* -/Y PRC slices exposed to picrotoxin or CGP55845 there was no increase in the magnitude of the afferent volley (Fig. 3E,G). Interestingly, we observed a significant increase in the magnitude of the synaptic response in *Cdkl5* -/Y PRC slices exposed to picrotoxin (Fig. 3F), but not to CGP55845 (Fig. 3H), suggesting that a GABAergic signaling inhibition, *via* $GABA_A$ receptors, induces an increase in the excitability of the *Cdkl5*-deficient neurons in PRC.

3.3. The $GABA_B$ receptor antagonist CGP55845 restored LTP magnitude in the perirhinal cortex of Cdkl5 -/Y mice

We recently showed that the magnitude of TBS-induced LTP is reduced in the PRC of *Cdkl5* -/Y mice (Ren et al., 2019). In order to examine whether excessive GABAergic inhibition might contribute to LTP impairment, we carried out experiments in which PRC slices from *Cdkl5* -/Y or +/Y mice were pharmacologically disinhibited by picrotoxin (100 μM), or CGP55845 (1 μM). As present experiments were carried out together with others, in which we evaluated the effect on LTP of another pharmacological treatment (Ren et al., 2019), LTP data

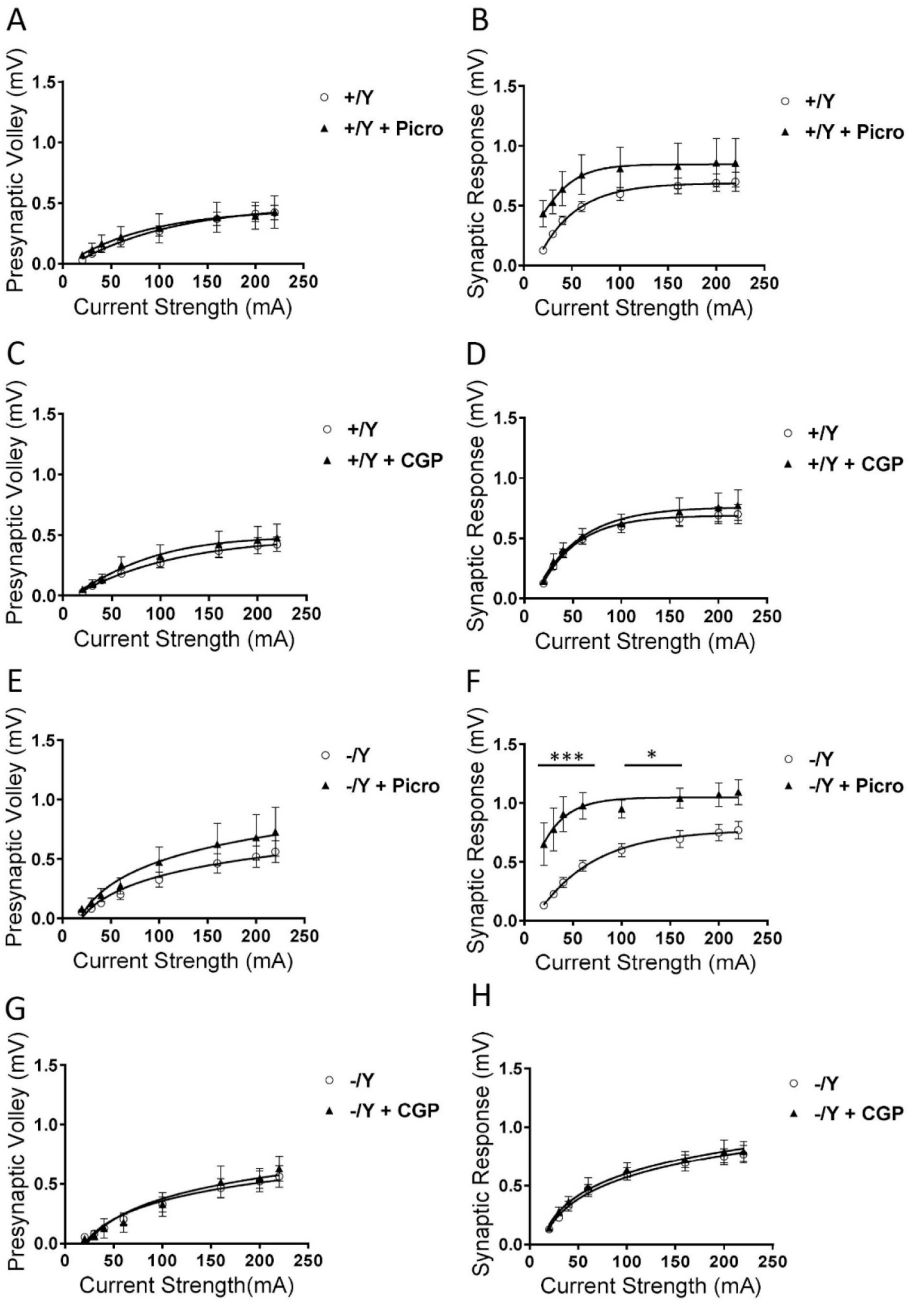

Fig. 3. Effect picrotoxin and CGP55845 on input-output relations in the perirhinal cortex of *Cdkl5* +/Y and *Cdkl5* -/Y mice (A,B) Magnitude of presynaptic volley (A) and synaptic response (B) evoked in layers II/III PRC as a function of stimulus strength in control slices ($n = 10$ slices from 8 mice) from *Cdkl5* +/Y mice and in picrotoxin (Picro; 100 μM)-treated slices ($n = 5$ slices from 4 mice) from *Cdkl5* +/Y mice. (C,D) Magnitude of presynaptic volley (C) and synaptic response (D) evoked in layers II/III PRC as a function of stimulus strength in control slices (n = 10 slices from 8 mice) from *Cdkl5* +/Y mice and in CGP55845 (CGP; 1 μM)-treated slices (n = 5 slices from 4 mice) from *Cdkl5* +/Y mice. (E,F) Magnitude of presynaptic volley (E) and synaptic response (F) evoked in layers II/III PRC as a function of stimulus strength in control slices ($n = 8$ slices from 8 mice) from *Cdkl5* -/Y mice and in picrotoxin-exposed slices (n = 5 slices from 5 mice) from *Cdkl5* -/Y mice. (G,H) Magnitude of presynaptic volley (G) and synaptic response (H) evoked in layers II/III PRC as a function of stimulus strength in control slices (n = 8 slices from 8 mice) from *Cdkl5* -/Y mice and CGP55845-exposed slices ($n = 4$ slices from 3 mice) from *Cdkl5* -/Y mice. Values represent mean ± SEM. $^{*}p < 0.05$, $^{***}p < 0.001$ (Tukey's LSD after 2-WAY ANOVA).

obtained in untreated *Cdkl5* -/Y and +/Y PRC slices are the same. Here we found that in both *Cdkl5* -/Y and +/Y PRC slices exposed to picrotoxin, the magnitude of LTP 55–60 min after TBS was lower in comparison with that of the corresponding untreated *Cdkl5* -/Y or +/Y PRC slices (Fig. 4A,B). In *Cdkl5* +/Y PRC slices treated with the selective inhibitor of $GABA_B$ receptors, CGP55845, the magnitude of LTP 55–60 min after TBS was similar to that of untreated *Cdkl5* +/Y PRC slices (Fig. 4C,D). Importantly, LTP magnitude was restored in *Cdkl5* -/Y PRC slices exposed to CGP55845 (Fig. 4C,D), suggesting that excessive inhibition mediated by $GABA_B$ receptors contributes to its impairment.

3.4. Altered NOR recognition memory in Cdkl5 -/Y mice is rescued by treatment with the $GABA_B$ receptor antagonist CGP55845

Balance between excitatory and inhibitory neurotransmission is a necessary pre-requisite for activity-dependent synaptic plasticity and, hence, efficient learning and memory. NOR memory refers to the ability to judge a previously encountered object as familiar and, in rodent brains, depends on the integrity of the PRC (Bussey et al., 2000; Bussey et al., 1999). We recently reported that this kind of memory, evaluated using the NOR test, is impaired in *Cdkl5* -/Y mice (Ren et al., 2019). As our electrophysiology data suggest that excessive inhibition mediated by $GABA_B$ receptors contributes to LTP impairment in PRC of *Cdkl5* -/Y mice, it is reasonable to hypothesize that it might also play a role in NOR memory impairment. To test this hypothesis, we investigated whether acute treatment with CGP55845 (0.5 mg/kg, i.p. injections 2 h before NOR test; Fig. 5A) could improve NOR in *Cdkl5* KO mice. A 4-object NOR test was performed in an open field arena, preceded by a 2-day habituation phase in the open field arena without objects. The NOR test started on the third day with a familiarization phase (10 min duration in the presence of 4 objects) followed, after a delay of 1 h (during which one of the four objects was replaced by a novel object), by the preference

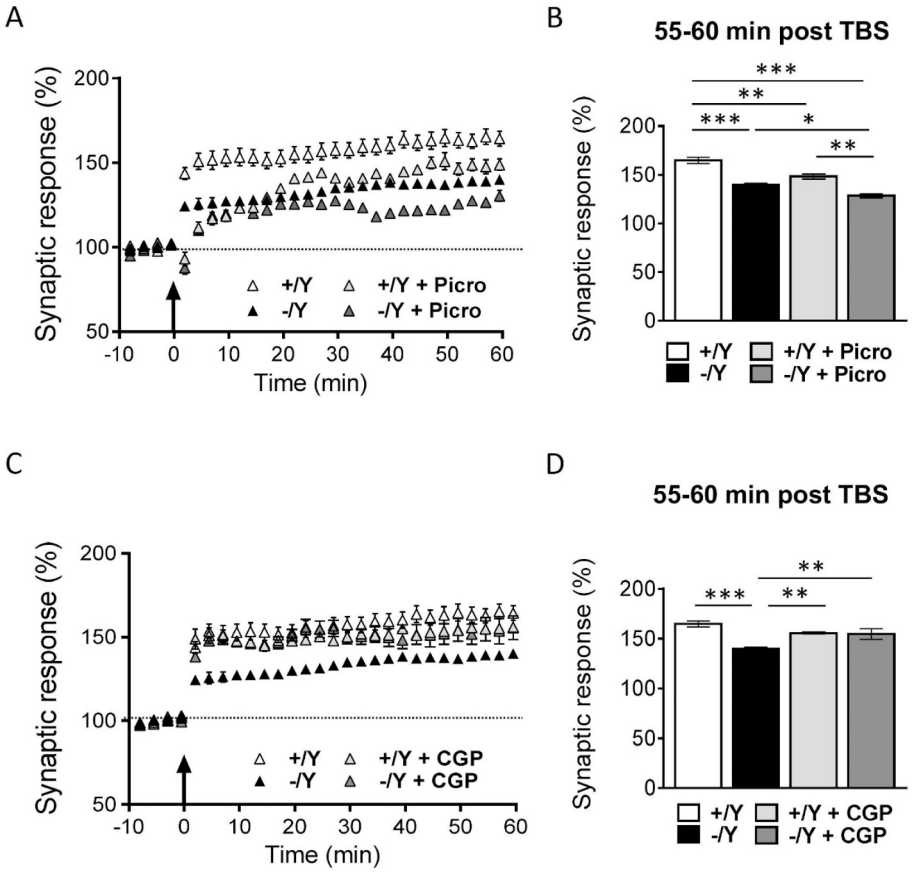

Fig. 4. Effect of picrotoxin and CGP55845 on LTP in the perirhinal cortex of *Cdkl5* +/Y and *Cdkl5* -/Y mice (A) Magnitude of TBS-induced LTP in layers II-III PRC of *Cdkl5* +/Y and *Cdkl5* -/Y control slices and slices exposed to picrotoxin (Picro; 100 μM). Here and in the following panels (B—D), the magnitude of the response is expressed as a percentage of the average amplitude of responses recorded 10 min before LTP induction. Here, and in panel C, the arrow indicates the time of TBS delivery. Recordings were carried out in control slices ($n = 9$ slices from 5 mice) from *Cdkl5* +/Y mice (+/Y), control slices ($n = 11$ slices from 5 mice) from *Cdkl5* -/Y mice (−/Y), picrotoxin-exposed slices (n = 5 slices from 3 mice) from *Cdkl5* +/Y mice (+/Y + Picro), and picrotoxin-exposed slices (n = 4 slices from 3 mice) from *Cdkl5* -/Y mice (−/Y + Picro). (B) Averaged magnitude of the responses recorded 55–60 min after TBS (same data as in (A)). (C) Magnitude of TBS-induced LTP in layers II-III PRC of *Cdkl5* +/Y and *Cdkl5* -/Y control slices and slices exposed to CGP55845 (CGP; 1 μM). Recordings were carried out in control slices (n = 9 slices from 5 mice) from *Cdkl5* +/Y mice (+/Y), control slices (n = 11 slices from 5 mice) from *Cdkl5* -/Y mice (−/Y), CGP55845-exposed slices (n = 4 slices from 2 mice) from *Cdkl5* +/Y mice (+/Y + CGP) and CGP55845-exposed slices (n = 5 slices from 3 mice) from *Cdkl5* -/Y mice (−/Y + CGP). (D) Averaged magnitude of the responses recorded 55–60 min after TBS (same data reported in (C)). Values represent mean ± SEM. *p < 0.05, **p < 0.01, ***p < 0.001 (Tukey's LSD after 2-WAY ANOVA).

test phase (10 min duration). CGP55845 was injected 2 h before the familiarization phase (Fig. 5A,B).

In line with our previous results (Ren et al., 2019), while all groups spent equal time exploring the four objects during the familiarization phase (Fig. 5C), vehicle-treated *Cdkl5* +/Y spent significantly more time exploring the novel object in the test phase, *i.e.* its preference index was significantly larger (Fig. 5D); but the preference index was similar for the four objects in vehicle-treated *Cdkl5* -/Y mice (Fig. 5D), indicating a deficit in remembering the identity of an object in an open field. Interestingly, treatment with CGP555845 rescued NOR memory in *Cdkl5* -/Y mice, whereas it impaired it in *Cdkl5* +/Y mice (Fig. 5D).

To monitor possible changes in spontaneous locomotion after treatment with CGP555845, the total distance traveled, and average velocity of movement were evaluated. *Cdkl5* -/Y mice showed a slightly reduced locomotor activity compared to *Cdkl5* +/Y mice (Supplementary Fig. 1). Interestingly, treatment with the $GABA_B$ receptor antagonist decreased spontaneous locomotor activity of both *Cdkl5* -/Y and +/Y mice (Supplementary Fig. 1A,B). These observations suggest that the physiological balance between excitation and inhibition is crucial for motor behavior, and that the reduced locomotor activity observed in *Cdkl5* -/Y mice is not due to excessive $GABA_B$ receptor-mediated signaling.

3.5. Impaired spine number and maturation and synaptic connectivity in Cdkl5 -/Y mice are improved by treatment with the $GABA_B$ receptor antagonist CGP55845

Enhancement of NOR memory by the $GABA_B$ receptor antagonist in *Cdkl5* -/Y mice can involve several mechanisms. We recently demonstrated that PRC neurons from *Cdkl5* mutant mice show several morphological alterations, including impaired spine density/maturation and impaired excitatory synaptic connectivity, as shown by a reduced number of PSD95 positive puncta (Ren et al., 2019). To evaluate whether the observed functional improvement is accompanied by a structural improvement, mice were sacrificed 4 h after treatment (Fig. 5A) to measure spine density/maturation and PSD95-positive puncta. Treatment with CGP55845 significantly improved the number of spines (Fig. 6A,B), as well as the balance between immature and mature spines (Fig. 6B,C) in the PRC of *Cdkl5* -/Y mice. Moreover, it caused a small but significant increase of PSD95 immunoreactive puncta in the PRC of *Cdkl5* -/Y mice (Fig. 6D,E). On the contrary, it had no effects on spine density (Fig. 6A,B) or maturation (Fig. 6B,C) in the PRC of *Cdkl5* +/Y mice, but significantly reduced the number of PSD95-positive puncta (Fig. 6D,E).

It was reported that $GABA_B$ antagonists increase brain levels of the brain-derived neurotrophic factor (BDNF) (Heese et al., 2000; Kleschevnikov et al., 2012), which is necessary for the formation and maturation of dendritic spines during postnatal development (Chapleau et al., 2009). To investigate the molecular mechanisms underlying the improvement of dendritic spine maturation, we examined BDNF levels in PRC homogenates of *Cdkl5* -/Y and +/Y mice following administration of vehicle or CGP55845. PRC samples were collected 2 h after treatment. Levels of BDNF were similar in *Cdkl5* -/Y and *Cdkl5* +/Y mice treated with the vehicle or CGP55845 (Supplementary Fig. 2). Thus, the molecular mechanism underlying CGP55845-induced effects on dendritic spines remains to be determined.

4. Discussion

An important characteristic of the clinical phenotype in CDD is intellectual disability and, in particular, impairment of learning and memory. Studies of mouse genetic models have revealed that deficient NOR and spatial memory in CDD could be a result of reduced synaptic plasticity (Ren et al., 2019; Tang et al., 2017), and that a decreased number and reduced efficacy of excitatory synapses could play a critical

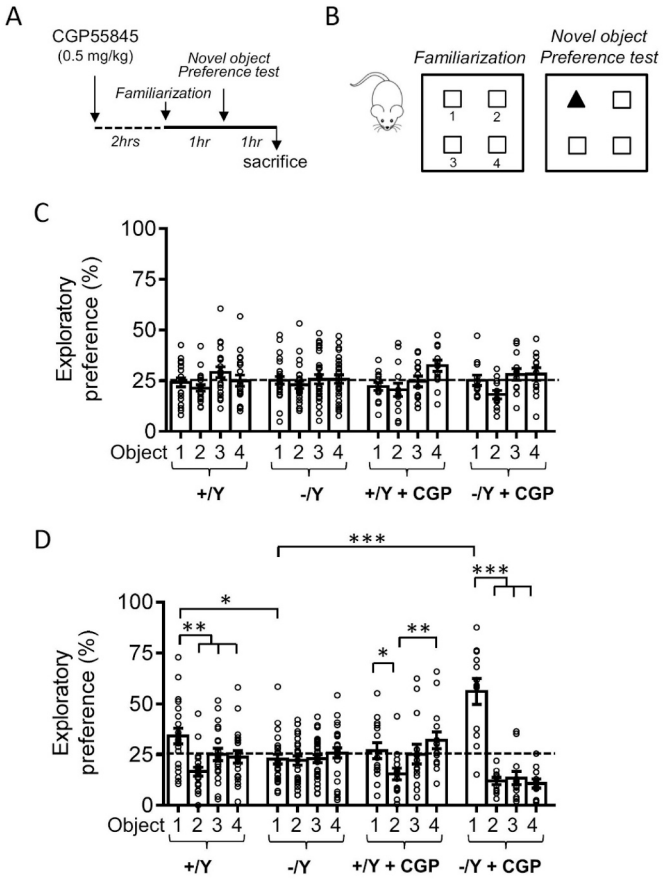

Fig. 5. Effect of treatment with CGP55845 on NOR memory in *Cdkl5* +/Y and *Cdkl5* -/Y mice (A,B) Experimental design for the NOR task. CGP55845 (0.5 mg/kg suspended in saline), or equivalent volume of saline only, was injected intraperitoneally in the mouse before the beginning of the familiarization phase, in which it was allowed to explore for 10 min four identical objects placed near the corners of a 50x50cm arena. After a delay of 1 h, during which one of the four objects (object 1) was replaced by a novel object, the animal was returned to the arena for the preference test phase (10 min duration). One hour later it was sacrificed for histological analyses. (C) Percentage of time spent exploring the four identical objects during the familiarization phase. Groups of mice: vehicle-treated *Cdkl5* +/Y (+/Y; $n = 20$ mice), vehicle-treated *Cdkl5* -/Y (−/Y; $n = 27$ mice), CGP55845-treated *Cdkl5* +/Y (+/Y + CGP; $n = 14$ mice), CGP55845-treated *Cdkl5* -/Y (−/Y + CGP; $n = 12$ mice) mice. (D) Percentage of time exploring the new object 1 and the previous identical objects 2–4 during the preference test phase (retention period of 1 h after familiarization). Same mice as in (C). Values represent mean ± SEM. *p < 0.05, **p < 0.01, ***p < 0.001 (Fisher's LSD after 2-WAY ANOVA).

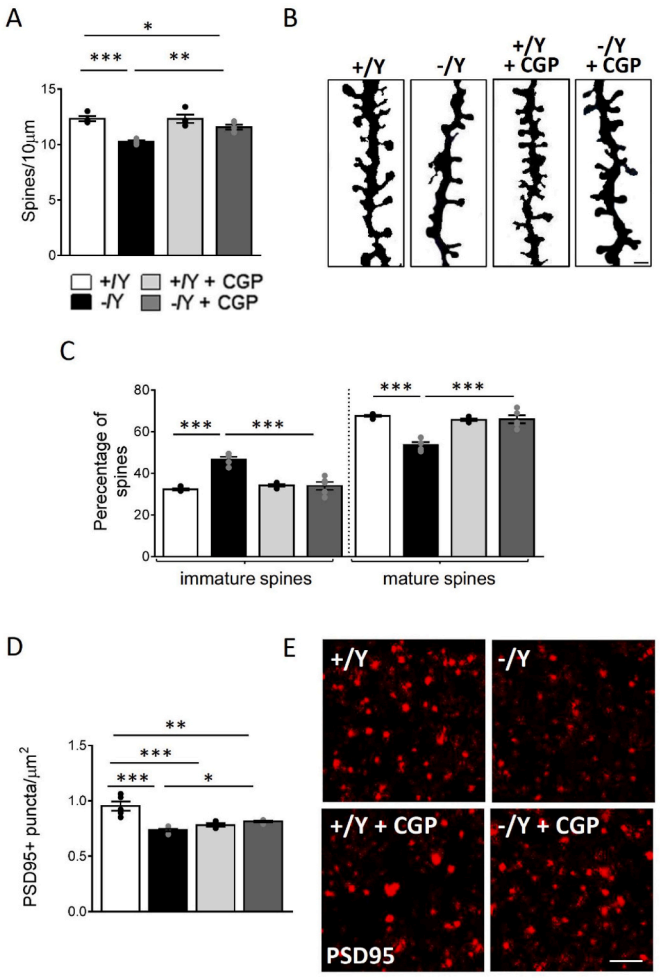

Fig. 6. Effects of treatment with CGP55845 on dendritic spines and synaptic connectivity in the perirhinal cortex of *Cdkl5* +/Y and *Cdkl5* -/Y mice (A) Dendritic spine density (number of spines per 10 µm) in apical dendrites of layer II-III PRC neurons of vehicle-treated (+/Y n = 4 mice; −/Y n = 4 mice) and CGP55845-treated (+/Y + CGP n = 4 mice; −/Y + CGP n = 5 mice) *Cdkl5* mice. (B) Examples of Golgi-stained apical dendritic branches of layer II-III PRC neurons of one animal from each experimental group. Scale bar = 1 µm. (C) Percentage of immature (filopodia, thin, and stubby-shaped) and mature (mushroom- and cup-shaped) spines in relation to the total number of protrusions in layer II-III PRC neurons in mice as in (A). (D) Number of PSD95 positive puncta per μm^2 in layer II-III of the PRC of vehicle-treated (+/Y n = 5 mice; −/Y n = 5 mice) and CGP55845-treated (+/Y + CGP n = 4 mice; −/Y + CGP n = 4 mice) *Cdkl5* mice. (E) Confocal images of PRC sections processed for PSD95 immunohistochemistry of one animal from each experimental group. Scale bar = 2 µm. Values represent mean ± SEM. *p < 0.05, **p < 0.01, ***p < 0.001 (Fisher's LSD after 2-WAY ANOVA).

role in these abnormalities (Della Sala et al., 2016; Pizzo et al., 2016; Ren et al., 2019). Here we present the first evidence that excessive inhibition mediated by $GABA_B$ receptors contributes to LTP impairment in PRC slices from *Cdkl5* KO mice. Moreover, acute *in vivo* treatment with the $GABA_B$ receptor antagonist CGP55845 restored NOR memory in these mice, increased the number of PSD95 positive puncta and normalized the morphology of dendritic spines in PRC.

An excess of inhibitory efficiency in the *Cdkl5* KO mouse model was first suggested based on histological studies in the primary visual cortex, that demonstrated increased density of parvalbumin-positive inhibitory neurons and immunoreactivity of the vesicular GABA transporter (VGAT), a protein selectively expressed in GABAergic axon terminals (Pizzo et al., 2016). Here we found a similar increase in the levels of VGAT in PRC of *Cdkl5* -/Y mice, suggesting that an excess of inhibition also occurs in this cortical area. Differently, no significant alterations in VGAT staining were described in the thalamus (Lupori et al., 2019), and a reduction of the GABA-related marker GAD67 was observed in the molecular layer of the cerebellum in *Cdkl5* -/Y mice (Sivilia et al., 2016), suggesting a region-specific effect of CDKL5 on GABAergic connectivity. In contrast, our findings showing that gephyrin, $GABA_B$ receptors, $GABA_A$ receptors, and GIRK2 levels are not different in the PRC between *Cdkl5* KO and wild-type mice, suggest that the absence of CDKL5 does not produce major effects on the organization of the inhibitory postsynaptic compartment. Interestingly, our current data are in line with previous findings showing that the density of gephyrin-positive puncta is unaffected in the primary visual cortex of *Cdkl5* mutant mice (Pizzo et al., 2016).

In line with the increased VGAT-positive pre-synaptic terminals, we found that input-output relation of glutamatergic synaptic transmission in the PRC of *Cdkl5* -/Y mice was affected by inhibition of $GABA_A$

receptors. The magnitude of the synaptic response significantly increased, whereas the afferent volley remained unchanged. The location of the stimulating electrode in the superficial layers of the PRC implies that electrode stimulation activated both local neurons as well as axon fibers of neurons projecting to this cortical region. Present data suggest that removal of $GABA_A$ receptor-mediated inhibition increases the excitation of PRC glutamatergic neurons located at the recording site, with a consequent increase in the size of the population of firing neurons, without affecting the excitability of the neurons whose fibers activate them. The increase of excitation of PRC glutamatergic neurons might depend on a stronger excitatory input that is needed to compensate the increased efficiency of GABAergic inhibition (increased number of VGAT-positive pre-synaptic terminals) and is unmasked when $GABA_A$ receptors are blocked by picrotoxin. Accordingly, picrotoxin had no effect on input-output relation of glutamatergic synaptic transmission in the PRC of *Cdkl5* +/Y mice, where the balance between inhibition and excitation is physiological. The observation that inhibition of $GABA_B$ receptors had no effect on the magnitude of the afferent volley or synaptic response in both *Cdkl5* -/Y and +/Y mice is not surprising, as they are coupled to G proteins and influence synaptic transmission over a slower timescale.

We have previously shown that the magnitude of TBS-induced LTP is reduced in the PRC of *Cdkl5* -/Y mice (Ren et al., 2019). The increased efficiency of the inhibitory connectivity observed in the present study suggests that one strategy to improve synaptic plasticity in the PRC of *Cdkl5* -/Y mice might be to reduce this inhibitory drive. Interestingly, we found that exposure to CGP55845 restored LTP magnitude in *Cdkl5* -/Y PRC slices (Fig. 4C,D), suggesting that excessive inhibition mediated by $GABA_B$ receptors contributes to its impairment. GABA can interact at both $GABA_B$ autoreceptors as well as at presynaptic and postsynaptic $GABA_B$ heteroreceptors in glutamatergic neurons (Gassmann and Bettler, 2012). The effect of $GABA_B$ receptor blockade on LTP suggests that the abnormality of the GABAergic system in the PRC of *Cdkl5* -/Y mice may include an imbalance towards a greater number of heteroreceptors on glutamatergic neurons. The mechanism underlying CGP55845-induced LTP restoration may include increase of glutamate release due to presynaptic $GABA_B$ receptor blockade, and increase of Ca^{2+} entry through NMDA glutamate receptors due to postsynaptic $GABA_B$ receptor blockade (Chalifoux and Carter, 2010; Morrisett et al., 1991). In line with this hypothesis and with a previous observation (Roncace et al., 2017), exposure to CGP55845 did not change the magnitude of LTP in the PRC of wild-type mice, where the balance between $GABA_B$ heteroreceptors and autoreceptors is physiological.

Exposure to the $GABA_A$ receptor blocker picrotoxin decreased LTP magnitude in the PRC in both wild-type ((Roncace et al., 2017) and present findings) and -/Y mice. This might be caused by disinhibition (*i.e.* blockade of $GABA_A$-mediated inhibition) of inhibitory interneurons that act on glutamatergic neurons through $GABA_B$ receptors. This hypothesis takes into account the apparent discrepancy that picrotoxin increased synaptic response only in -/Y mice, whereas it decreased LTP in both -/Y and +/Y mice. Being based on inhibition mediated by $GABA_B$ receptors, the above reported disinhibition can only be effective on synaptic plasticity, due to the slow timescale of its effects.

Interestingly, we found that impaired PRC-dependent NOR memory is rescued by acute treatment with the $GABA_B$ receptor antagonist CGP55845. This finding is fully in line with our evidence showing that treatment with CGP55845 restored LTP and increased the number of PSD95 positive puncta as well as the number and maturation of dendritic spines in *Cdkl5* -/Y mice PRC. The structural changes observed just 4 h after treatment with CGP55845 in the dendrites are consistent with those observed within an hour during LTP *in vitro* (Engert and Bonhoeffer, 1999; Toni et al., 1999), and in the living brain during learning (Xu et al., 2009). Moreover, it has been shown that PSD-95 accumulation in spines occurs within a few minutes to hours after initial contact between the nascent spine and a presynaptic partner in neuronal cultures (Bresler et al., 2001; Friedman et al., 2000; Okabe et al., 2001). Besides these improvements, it is reasonable to suppose that additional effects occurring in PRC and in other brain regions may contribute to the effect on memory of $GABA_B$ receptor inhibition. In contrast to the effects observed in *Cdkl5* KO mice, memory performance of wild-type mice worsened and the density of PSD95 positive synaptic puncta decreased after CGP55845 administration. Although not in agreement with a previous observation (Kleschevnikov et al., 2012), this result is not surprising, as the performance of wild-type mice is based on the physiological balance between excitation and inhibition. Indeed, our results indicate that alterations of this balance, resulting from either increase or decrease of $GABA_B$ receptor-mediated inhibition, lead to deterioration of memory performance.

Taken together, present findings suggest that inhibition of excessive $GABA_B$ receptor-mediated signaling efficiently improves synaptic plasticity and memory in a mouse model of CDKL5 deficiency.

Authors' contributions

LG and *CF* performed experiments, analyzed data, and contributed to the draft of the paper; ST performed experiments and analyzed data; VR designed and performed electrophysiological experiments and analyzed data; ML, YA, GG, ACB, GM, MT and ER performed experiments; RR designed and supervised the behavioral study; MG supervised part of the immunohistochemical study; GA designed and supervised the electrophysiological study, and contributed to the draft of the paper; EC designed the study, analyzed data, and drafted the paper.

Credit author statement

Laura Gennaccaro, Claudia Fuchs and Vincenzo Roncacè: collected the data and contributed to the study design; Stefania Trazzi, Manuela Loi, Yassine Ait-Bali, Giuseppe Galvani, Anna Cecilia Berardi, Giorgio Medici, Marianna Tassinari and Eisa Ren: collected the data; Roberto Rimondini: supervised the behavioral study; Maurizio Giustetto: supervised part of the immunohistochemical study; Giorgio Aicardi: designed and supervised the electrophysiological study, and contributed to the draft of the paper; Elisabetta Ciani: designed the study, analyzed data, and drafted the paper.

Declaration of competing interest

All authors reported no biomedical financial interests or potential conflicts of interest.

Acknowledgments

This work was supported by the Telethon foundation [grant number GGP19045 to EC and MG], and by the Italian parent associations "CDKL5 insieme verso la cura" (EC and MG) and "L'albero di Greta" (MG), by the Association Française du syndrome de Rett (MG) and the International Foundation for CDKL5 Research (MG).

Appendix A. Supplementary data

Supplementary data to this article can be found online at https://doi.org/10.1016/j.nbd.2021.105304.

References

Aicardi, G., et al., 2004. Induction of long-term potentiation and depression is reflected by corresponding changes in secretion of endogenous brain-derived neurotrophic factor. Proc. Natl. Acad. Sci. U. S. A. 101, 15788–15792.

Amendola, E., et al., 2014. Mapping pathological phenotypes in a mouse model of CDKL5 disorder. PLoS One 9, e91613.

Bertani, I., et al., 2006. Functional consequences of mutations in CDKL5, an X-linked gene involved in infantile spasms and mental retardation. J. Biol. Chem. 281, 32048–32056.

Bradford, M.M., 1976. A rapid and sensitive method for the quantitation of microgram quantities of protein utilizing the principle of protein-dye binding. Anal. Biochem. 72, 248–254.
Bresler, T., et al., 2001. The dynamics of SAP90/PSD-95 recruitment to new synaptic junctions. Mol. Cell. Neurosci. 18, 149–167.
Brown, M.W., Aggleton, J.P., 2001. Recognition memory: what are the roles of the perirhinal cortex and hippocampus? Nat. Rev. Neurosci. 2, 51–61.
Bussey, T.J., et al., 1999. Functionally dissociating aspects of event memory: the effects of combined perirhinal and postrhinal cortex lesions on object and place memory in the rat. J. Neurosci. 19, 495–502.
Bussey, T.J., et al., 2000. Distinct patterns of behavioural impairments resulting from fornix transection or neurotoxic lesions of the perirhinal and postrhinal cortices in the rat. Behav. Brain Res. 111, 187–202.
Chalifoux, J.R., Carter, A.G., 2010. GABAB receptors modulate NMDA receptor calcium signals in dendritic spines. Neuron. 66, 101–113.
Chapleau, C.A., et al., 2009. Dendritic spine pathologies in hippocampal pyramidal neurons from Rett syndrome brain and after expression of Rett-associated MECP2 mutations. Neurobiol. Dis. 35, 219–233.
Chaudhry, F.A., et al., 1998. The vesicular GABA transporter, VGAT, localizes to synaptic vesicles in sets of glycinergic as well as GABAergic neurons. J. Neurosci. 18, 9733–9750.
Chen, Q., et al., 2010. CDKL5, a protein associated with rett syndrome, regulates neuronal morphogenesis via Rac1 signaling. J. Neurosci. 30, 12777–12786.
Choii, G., Ko, J., 2015. Gephyrin: a central GABAergic synapse organizer. Exp. Mol. Med. 47, e158.
Della Sala, G., et al., 2016. Dendritic spine instability in a mouse model of CDKL5 disorder is rescued by insulin-like growth factor 1. Biol. Psychiatry 80, 302–311.
Demarest, S., et al., 2019a. Severity assessment in CDKL5 deficiency disorder. Pediatr. Neurol. 97, 38–42.
Demarest, S.T., et al., 2019b. CDKL5 deficiency disorder: relationship between genotype, epilepsy, cortical visual impairment, and development. Epilepsia. 60, 1733–1742.
Engert, F., Bonhoeffer, T., 1999. Dendritic spine changes associated with hippocampal long-term synaptic plasticity. Nature. 399, 66–70.
Fehr, S., et al., 2013. The CDKL5 disorder is an independent clinical entity associated with early-onset encephalopathy. Eur. J. Hum. Genet. 21, 266–273.
Friedman, H.V., et al., 2000. Assembly of new individual excitatory synapses: time course and temporal order of synaptic molecule recruitment. Neuron. 27, 57–69.
Fuchs, C., et al., 2014. Loss of CDKL5 impairs survival and dendritic growth of newborn neurons by altering AKT/GSK-3beta signaling. Neurobiol. Dis. 70, 53–68.
Fuchs, C., et al., 2015. Inhibition of GSK3beta rescues hippocampal development and learning in a mouse model of CDKL5 disorder. Neurobiol. Dis. 82, 298–310.
Garden, D.L., et al., 2002. Differences in GABAergic transmission between two inputs into the perirhinal cortex. Eur. J. Neurosci. 16, 437–444.
Gassmann, M., Bettler, B., 2012. Regulation of neuronal GABA(B) receptor functions by subunit composition. Nat. Rev. Neurosci. 13, 380–394.
Guerrini, R., Parrini, E., 2012. Epilepsy in Rett syndrome, and CDKL5- and FOXG1-gene-related encephalopathies. Epilepsia 53, 2067–2078.
Hector, R.D., et al., 2016. Characterisation of CDKL5 transcript isoforms in human and mouse. PLoS One 11, e0157758.
Heese, K., et al., 2000. GABA(B) receptor antagonists elevate both mRNA and protein levels of the neurotrophins nerve growth factor (NGF) and brain-derived neurotrophic factor (BDNF) but not neurotrophin-3 (NT-3) in brain and spinal cord of rats. Neuropharmacology. 39, 449–462.
Kleschevnikov, A.M., et al., 2012. Deficits in cognition and synaptic plasticity in a mouse model of down syndrome ameliorated by GABAB receptor antagonists. J. Neurosci. 32, 9217–9227.
Livak, K.J., Schmittgen, T.D., 2001. Analysis of relative gene expression data using real-time quantitative PCR and the 2(-Delta Delta C(T)) method. Methods 25, 402–408.
Lo Martire, V., et al., 2017. CDKL5 deficiency entails sleep apneas in mice. J. Sleep Res. 26, 495–497.
Lupori, L., et al., 2019. Site-specific abnormalities in the visual system of a mouse model of CDKL5 deficiency disorder. Hum. Mol. Genet. 28, 2851–2861.
Mari, F., et al., 2005. CDKL5 belongs to the same molecular pathway of MeCP2 and it is responsible for the early-onset seizure variant of Rett syndrome. Hum. Mol. Genet. 14, 1935–1946.
Mazziotti, R., et al., 2017. Searching for biomarkers of CDKL5 disorder: early-onset visual impairment in CDKL5 mutant mice. Hum. Mol. Genet. 26, 2290–2298.
Montini, E., et al., 1998. Identification and characterization of a novel serine-threonine kinase gene from the Xp22 region. Genomics 51, 427–433.
Morrisett, R.A., et al., 1991. GABAB-receptor-mediated inhibition of the N-methyl-D-aspartate component of synaptic transmission in the rat hippocampus. J. Neurosci. 11, 203–209.
Nawaz, M.S., et al., 2016. CDKL5 and Shootin1 interact and concur in regulating neuronal polarization. PLoS One 11, e0148634.
Okabe, S., et al., 2001. Rapid redistribution of the postsynaptic density protein PSD-Zip45 (Homer 1c) and its differential regulation by NMDA receptors and calcium channels. J. Neurosci. 21, 9561–9571.
Okuda, K., et al., 2017. CDKL5 controls postsynaptic localization of GluN2B-containing NMDA receptors in the hippocampus and regulates seizure susceptibility. Neurobiol. Dis. 106, 158–170.
Pizzo, R., et al., 2016. Lack of Cdkl5 disrupts the organization of excitatory and inhibitory synapses and parvalbumin interneurons in the primary visual cortex. Front. Cell. Neurosci. 10, 261.
Pizzo, R., et al., 1 October 2020. Structural bases of atypical whisker responses in a mouse model of CDKL5 deficiency disorder. Neuroscience 445, 130–143.
Ren, E., et al., 2019. Functional and structural impairments in the perirhinal cortex of a mouse model of CDKL5 deficiency disorder are rescued by a TrkB agonist. Front. Cell. Neurosci. 13, 169.
Ricciardi, S., et al., 2012. CDKL5 ensures excitatory synapse stability by reinforcing NGL-1-PSD95 interaction in the postsynaptic compartment and is impaired in patient iPSC-derived neurons. Nat. Cell Biol. 14, 911–923.
Roncace, V., et al., 2017. Neuroanatomical alterations and synaptic plasticity impairment in the perirhinal cortex of the Ts65Dn mouse model of down syndrome. Neurobiol. Dis. 106, 89–100.
Rusconi, L., et al., 2008. CDKL5 expression is modulated during neuronal development and its subcellular distribution is tightly regulated by the C-terminal tail. J. Biol. Chem. 283, 30101–30111.
Sivilia, S., et al., 2016. CDKL5 knockout leads to altered inhibitory transmission in the cerebellum of adult mice. Genes Brain Behav. 15, 491–502.
Tang, S., et al., 2017. Loss of CDKL5 in glutamatergic neurons disrupts hippocampal microcircuitry and leads to memory impairment in mice. J. Neurosci. 37, 7420–7437.
Terunuma, M., et al., 2014. Postsynaptic GABAB receptor activity regulates excitatory neuronal architecture and spatial memory. J. Neurosci. 34, 804–816.
Toni, N., et al., 1999. LTP promotes formation of multiple spine synapses between a single axon terminal and a dendrite. Nature 402, 421–425.
Trazzi, S., et al., 2014. APP-dependent alteration of GSK3beta activity impairs neurogenesis in the Ts65Dn mouse model of down syndrome. Neurobiol. Dis. 67, 24–36.
Trazzi, S., et al., 2016. HDAC4: a key factor underlying brain developmental alterations in CDKL5 disorder. Hum. Mol. Genet. 25, 3887–3907.
Trazzi, S., et al., 2018. CDKL5 protein substitution therapy rescues neurological phenotypes of a mouse model of CDKL5 disorder. Hum. Mol. Genet. 27, 1572–1592.
Wang, I.T., et al., 2012. Loss of CDKL5 disrupts kinome profile and event-related potentials leading to autistic-like phenotypes in mice. Proc. Natl. Acad. Sci. U. S. A. 109, 21516–21521.
Xu, T., et al., 2009. Rapid formation and selective stabilization of synapses for enduring motor memories. Nature 462, 915–919.
Ziakopoulos, Z., et al., 2000. GABAB receptors mediate frequency-dependent depression of excitatory potentials in rat perirhinal cortex in vitro. Eur. J. Neurosci. 12, 803–809.